

# Iron, nickel and zinc stoichiometric influences on the dynamic magneto-elastic properties of spinel ferrites

V. Grimal<sup>a,b,\*</sup>, D. Autissier<sup>b</sup>, L. Longuet<sup>b</sup>, H. Pascard<sup>c</sup>, M. Gervais<sup>a</sup>

<sup>a</sup> UMR 6157 CNRS-CEA LEMA, Université François Rabelais, Parc de Grandmont, 37000 Tours, France

<sup>b</sup> CEA/Le Ripault, BP 16, Monts, France

<sup>c</sup> Ecole Polytechnique, LSI, 91128 Palaiseau, France

Received 25 July 2005; received in revised form 15 October 2005; accepted 23 October 2005

Available online 15 December 2005

## Abstract

The influence of iron, nickel and zinc stoichiometry on dynamic magneto-elastic properties of  $\text{Ni}_{0.5}\text{Zn}_{0.5}\text{Fe}_2\text{O}_4$  spinel ferrites has been studied. The lattice parameters and the Curie temperatures were accurately measured. Both depend linearly on the iron, nickel and zinc stoichiometry and a linear relation was found between these two parameters. An ionic model is proposed. The effect of the stress on the magnetic dynamic permeability on polycrystalline toroidal samples is evaluated through measurements in a coaxial wave guide between 1 MHz and 6 GHz and with an applied stress in the range 0–20 MPa. The stress is applied along the torus axis. This materials family has a negative magnetostriction coefficient. Increasing the stress and the permeability drastically decreases at low frequencies (wall displacement) and increases at higher frequencies (gyromagnetism). The most important effect is observed for stoichiometric material. All the results could be consistently explained in terms of variation of anisotropy. © 2005 Elsevier Ltd. All rights reserved.

**Keywords:** Magnetic properties; Ferrites and soft magnets;  $(\text{Ni}, \text{Zn})\text{Fe}_2\text{O}_4$

## 1. Introduction

Physical and chemical properties of spinel ferrites change with the material stoichiometry. An ionic model is established to understand the results.

The  $\text{Ni}_{0.5}\text{Zn}_{0.5}\text{Fe}_2\text{O}_4$  spinel ferrites are sensitive to magnetostriction. Some fabrication parameters can influence drastically the magnetic properties and particularly the hyper-frequency magneto-elastic ones. For microwave applications, where stresses could be applied while assembling, it is necessary to understand those phenomenon. Behaviour in high frequency of Ni–Zn ferrite stoichiometry with a mechanic pressure has been studied previously in cylindrical sample<sup>1</sup> and toroidal sample<sup>2</sup> in narrow frequency band and without physical explanation. In this paper, we observe the effect of iron, nickel and zinc stoichiometry on magnetic properties. Some publications deal with magnetic static properties of Ni–Zn ferrite stoichiometry.<sup>3,4</sup> We present a complete study of

the magnetic behaviour in low and high frequencies in Ni–Zn ferrite, in relation to stoichiometry, with applied stresses.

## 2. Statics results

### 2.1. Materials synthesis and characterization

The materials have been prepared by a classical ceramic method: powder synthesis, pressing and sintering. The powders were synthesized by calcining a mixture of oxides ( $\text{Fe}_2\text{O}_3$ , NiO and ZnO) at 1050 °C for 3 h, in order to form the spinel phase. A wet grinding step with iron balls is used to increase the powder reactivity. The samples were shaped by cold isostatic pressing under 150 MPa. The densification was achieved by an air sintering for 15 h, at 1150 °C for iron stoichiometry study and at 1250 °C for nickel and zinc stoichiometry study.

To study stoichiometric effect, we have introduced more or less iron, nickel or zinc. To this aim, the following compositions (Table 1) were studied.

The materials microstructure appears to be independent of the stoichiometry.<sup>5</sup> The average grain size is close to 3  $\mu\text{m}$  (Fig. 1)

\* Corresponding author.

E-mail address: [virginie.grimal@wanadoo.fr](mailto:virginie.grimal@wanadoo.fr) (V. Grimal).

Table 1  
Final composition of studied materials determined by electron microprobe analysis

Iron stoichiometric effect	$\text{Ni}_{0.5}\text{Zn}_{0.5}\text{Fe}_{1.92}\text{O}_{4\pm\delta}$ $\text{Ni}_{0.5}\text{Zn}_{0.5}\text{Fe}_2\text{O}_{4\pm\delta}$	$\text{Ni}_{0.5}\text{Zn}_{0.5}\text{Fe}_{1.94}\text{O}_{4\pm\delta}$ $\text{Ni}_{0.5}\text{Zn}_{0.5}\text{Fe}_{2.02}\text{O}_{4\pm\delta}$	$\text{Ni}_{0.5}\text{Zn}_{0.5}\text{Fe}_{1.96}\text{O}_{4\pm\delta}$ $\text{Ni}_{0.5}\text{Zn}_{0.5}\text{Fe}_{2.04}\text{O}_{4\pm\delta}$	$\text{Ni}_{0.5}\text{Zn}_{0.5}\text{Fe}_{1.98}\text{O}_{4\pm\delta}$ $\text{Ni}_{0.5}\text{Zn}_{0.5}\text{Fe}_{2.06}\text{O}_{4\pm\delta}$
Nickel stoichiometric effect	$\text{Ni}_{0.48}\text{Zn}_{0.5}\text{Fe}_2\text{O}_{4\pm\delta}$	$\text{Ni}_{0.5}\text{Zn}_{0.5}\text{Fe}_2\text{O}_{4\pm\delta}$	$\text{Ni}_{0.52}\text{Zn}_{0.5}\text{Fe}_2\text{O}_{4\pm\delta}$	
Zinc stoichiometric effect	$\text{Ni}_{0.5}\text{Zn}_{0.48}\text{Fe}_2\text{O}_{4\pm\delta}$	$\text{Ni}_{0.5}\text{Zn}_{0.5}\text{Fe}_2\text{O}_{4\pm\delta}$	$\text{Ni}_{0.5}\text{Zn}_{0.52}\text{Fe}_2\text{O}_{4\pm\delta}$	

and the density represents 98% of the theoretical density. Electron microprobe analysis (Fig. 2) shows very small amounts of a secondary phase enriched in nickel and weakened in iron in addition to the spinel phase.

The lattice parameters were determined by X-ray diffraction. We can observe that lattice parameter decreases with the increase of iron stoichiometry (Fig. 3) and nickel stoichiometry (Fig. 4) but increases with zinc stoichiometry (Fig. 5).

For the stoichiometric material, the lattice parameter value is 8.3941 Å.

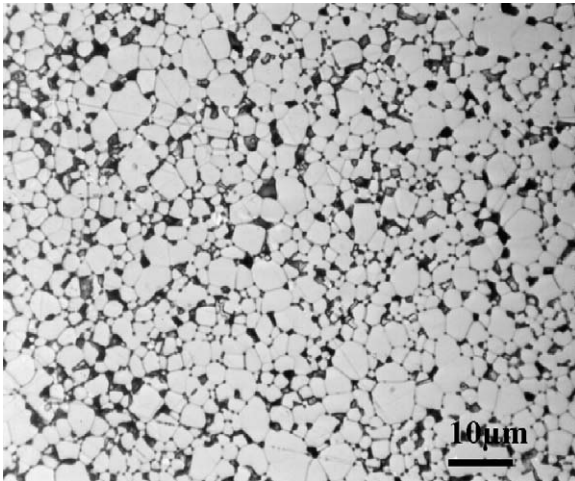


Fig. 1.  $\text{Ni}_{0.5}\text{Zn}_{0.5}\text{Fe}_2\text{O}_4$  sintered at 1150 °C observed by optical microscopy.

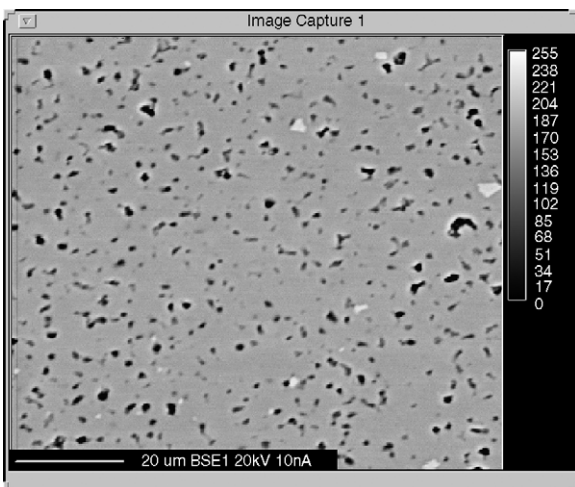


Fig. 2.  $\text{Ni}_{0.5}\text{Zn}_{0.5}\text{Fe}_2\text{O}_4$  sintered at 1150 °C observed by electron microprobe analysis.

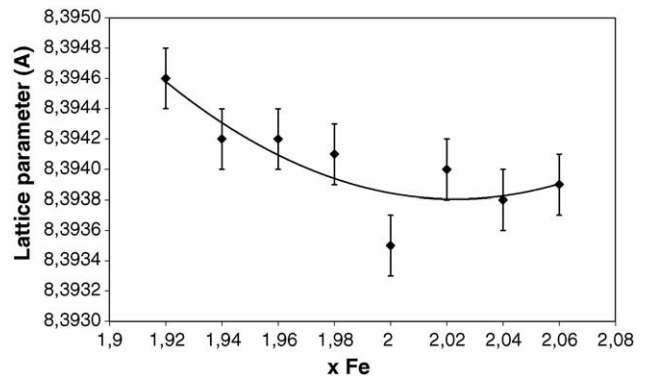


Fig. 3. Lattice parameter evolution vs. iron stoichiometry,  $\text{Ni}_{0.5}\text{Zn}_{0.5}\text{Fe}_x\text{O}_{4\pm\delta}$  sintered at 1150 °C.

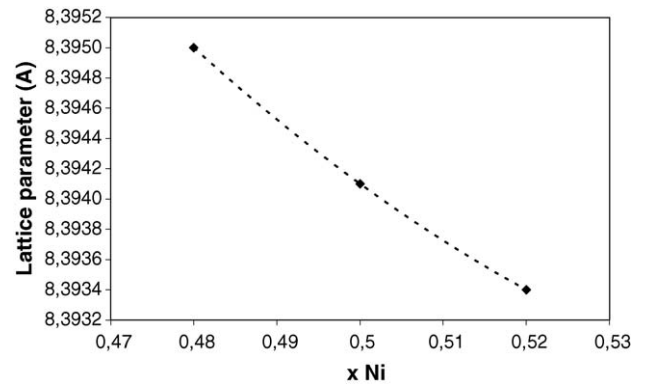


Fig. 4. Lattice parameter evolution vs. nickel stoichiometry,  $\text{Ni}_x\text{Zn}_{0.5}\text{Fe}_2\text{O}_{4\pm\delta}$  sintered at 1250 °C.

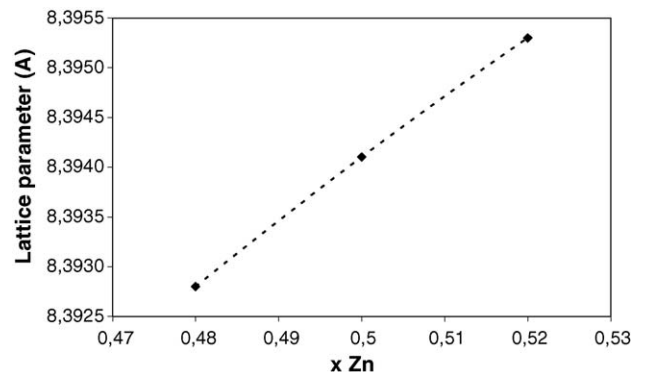


Fig. 5. Lattice parameter evolution vs. zinc stoichiometry,  $\text{Ni}_{0.5}\text{Zn}_x\text{Fe}_2\text{O}_{4\pm\delta}$  sintered at 1250 °C.

### 3. Ionic interpretation

According to those results, we can imagine an original ionic model. In spinel ferrites, there are 64 tetrahedral sites (sites A) whose only 8 are occupied and 32 octahedral sites (sites B) whose 16 are occupied. Sites A are smaller than sites B. In the nickel–zinc ferrite, nickel ions are located in sites B and zinc ions, in site A. Iron ions are split in sites A and B.

Fig. 3 shows for that the lattice parameter decreases when iron increases. In fact, iron ions move to sites A because they are more lacunary. Sites A being smaller than sites B, the lattice parameter decreases. Fig. 4 shows that when nickel ions are added, the lattice parameter decreases. In fact, we push iron ions from sites B to sites A so, the lattice parameter decreases. Fig. 5 shows that when zinc ions are added, lattice parameter increases. We can easily imagine that we push iron ions from sites A to sites B and sites B being larger than sites A, lattice increases.

#### 3.1. Magnetic measurements-static permeability measurements versus temperature

The initial permeability has been measured at 500 Hz in temperature from 295 to 600 K. Iron, nickel or zinc stoichiometry changes drastically the Curie temperature and the initial permeability of materials. Fig. 6a and b shows results.

For an over-stoichiometry ( $\text{Ni}_{0.52}\text{Zn}_{0.5}\text{Fe}_2\text{O}_4$  and  $\text{Ni}_{0.5}\text{Zn}_{0.52}\text{Fe}_2\text{O}_4$ ), permeability systematically decreases (Fig. 6a) and for iron stoichiometry, we have a maximum for the stoichiometric material (Fig. 6b).

For iron (Fig. 7), the Curie temperature increases when iron stoichiometry increases. This is in agreement with ref.<sup>5</sup>.

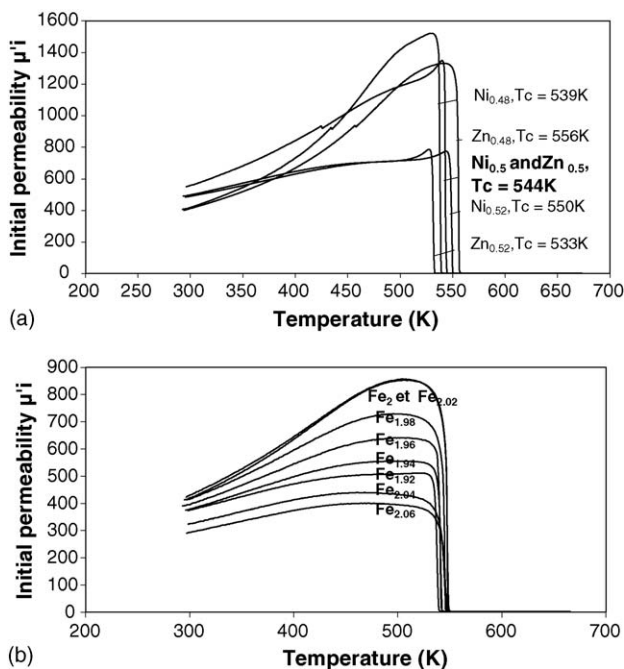


Fig. 6. (a) Initial permeability measured at 500 Hz on toroidal sample for different nickel and zinc stoichiometries vs. temperature. (b) Initial permeability measured at 500 Hz on toroidal sample for different iron stoichiometry vs. temperature.

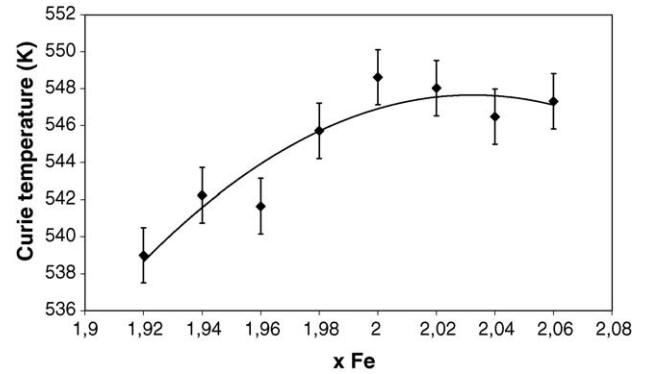


Fig. 7. Curie temperature vs. iron stoichiometry,  $\text{Ni}_{0.5}\text{Zn}_{0.5}\text{Fe}_x\text{O}_{4\pm\delta}$  sintered at  $1150^\circ\text{C}$ .

For nickel, the Curie temperature increases with the increase of nickel stoichiometry (Fig. 8a) while for zinc, it decreases (Fig. 8b).

In this low frequency area, the permeability is mainly due to the displacement of the magnetic walls, regulated by (1) the magnetization, (2) the anisotropy and (3) the distance between pinning point of walls (grain boundaries, porosities). The magnetization shows only little variations (between 59 and 64 uem/g) and the microstructure is independent of the stoichiometry (Section 1): the variations of the permeability are probably due to the variation of the anisotropy (the iron changes of site when changing Ni and Zn stoichiometry).

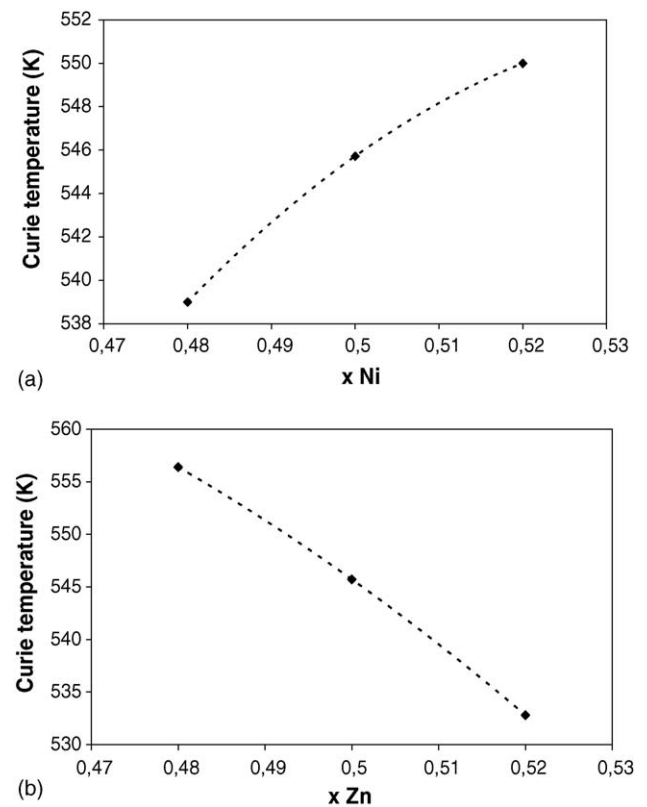


Fig. 8. (a) Curie temperature vs. nickel stoichiometry,  $\text{Ni}_x\text{Zn}_{0.5}\text{Fe}_2\text{O}_{4\pm\delta}$  sintered at  $1250^\circ\text{C}$ . (b) Curie temperature vs. zinc stoichiometry,  $\text{Ni}_{0.5}\text{Zn}_x\text{Fe}_2\text{O}_{4\pm\delta}$  sintered at  $1250^\circ\text{C}$ .

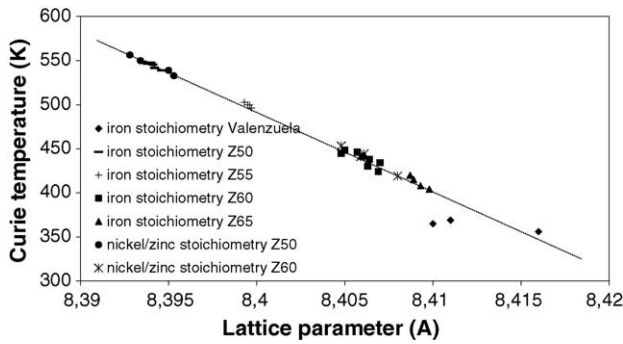


Fig. 9. Curie temperature vs. lattice parameter for different compositions:  $\text{Ni}_{0,5}\text{Zn}_{0,5}\text{Fe}_2\text{O}_4$  (Z50),  $\text{Ni}_{0,45}\text{Zn}_{0,55}\text{Fe}_2\text{O}_4$  (Z55),  $\text{Ni}_{0,4}\text{Zn}_{0,6}\text{Fe}_2\text{O}_4$  (Z60),  $\text{Ni}_{0,35}\text{Zn}_{0,65}\text{Fe}_2\text{O}_4$  (Z65),  $\text{Ni}_{0,3}\text{Zn}_{0,7}\text{Fe}_2\text{O}_4$  (Valenzuela).

The plot of the lattice parameter versus the Curie temperature for all the different compositions versus iron, nickel and zinc stoichiometry shows a linear relation (Fig. 9). In order to complete this study, we have reported Valenzuela<sup>5</sup> results and we have elaborated others compositions (Z50: reference material,  $\text{Ni}_{0,5}\text{Zn}_{0,5}\text{Fe}_2\text{O}_4$ ; Z55:  $\text{Ni}_{0,45}\text{Zn}_{0,55}\text{Fe}_2\text{O}_4$ ; Z60:  $\text{Ni}_{0,4}\text{Zn}_{0,6}\text{Fe}_2\text{O}_4$  and Z65:  $\text{Ni}_{0,35}\text{Zn}_{0,65}\text{Fe}_2\text{O}_4$ ) with identical iron stoichiometry variations.

A linear relation between the lattice parameter and the Curie temperature can be observed for all compositions, independent of iron, nickel and zinc stoichiometry. In first approach, we can consider a linear dependence of the Curie temperature versus the exchange energy<sup>6</sup>; on the other hand the exchange energy has an electrostatic origin and therefore depends on distance between ions, expressed by lattice parameter.

## 4. Dynamics results

### 4.1. Dynamic permeability measurements versus frequency

The frequency variations of the permeability has been measured using a HP 8753D network analyzer on polycrystalline

toroidal samples, in a coaxial wave guide at the APC7 standard between 1 and 6 MHz, at room temperature. The Fig. 10 shows the permeability and the permittivity versus frequency evolution for the different iron stoichiometry.

We can observe the two permeability contributions (Fig. 10a), i.e. gyromagnetism at higher frequencies and wall moving at lower frequencies; they are not well separated. The permeability increases from  $x=1.92$  to 2 and decreases from  $x=2$  to 2.06. Those materials do not have any dielectric losses as far as they are sintered at low temperature (Fig. 10b).

In contrast, nickel and zinc stoichiometry studies shows that those materials have dielectric losses (Fig. 11). Materials under-stoichiometric in nickel or zinc have important losses, probably due to the apparition of divalent iron, in order to maintain the electric equilibrium.

### 4.2. Dynamic permeability measurements versus frequency and stress

The frequency variations of the permeability under stress has been measured using a HP 8753D network analyzer on polycrystalline toroidal samples, in a coaxial wave guide at the APC7 standard between 1 and 6 MHz, at room temperature and with applied stresses between 0 and 20 MPa. The Fig. 12 shows, for example the results for  $\text{Ni}_{0,5}\text{Zn}_{0,5}\text{Fe}_2\text{O}_4$  with an iron stoichiometry of  $x=1.98$ .

The stress is applied along the torus axis with a micrometer setscrew, and measured with the help of a strength sensor. We can observe a different effect on the two permeability contributions. At lower frequencies, permeability decreases with applied stress whereas at higher frequencies, it increases. Those observations were valuable for all materials of this study. We can explain this phenomenon in term of magnetization for wall moving and in term of anisotropy for gyromagnetism.<sup>7</sup> Concerning the wall bulging area, we can explain the permeability behavior in term of anisotropy. The magnetization and the anisotropy field in a torus are aligned circularly. When a stress is applied perpendicularly to

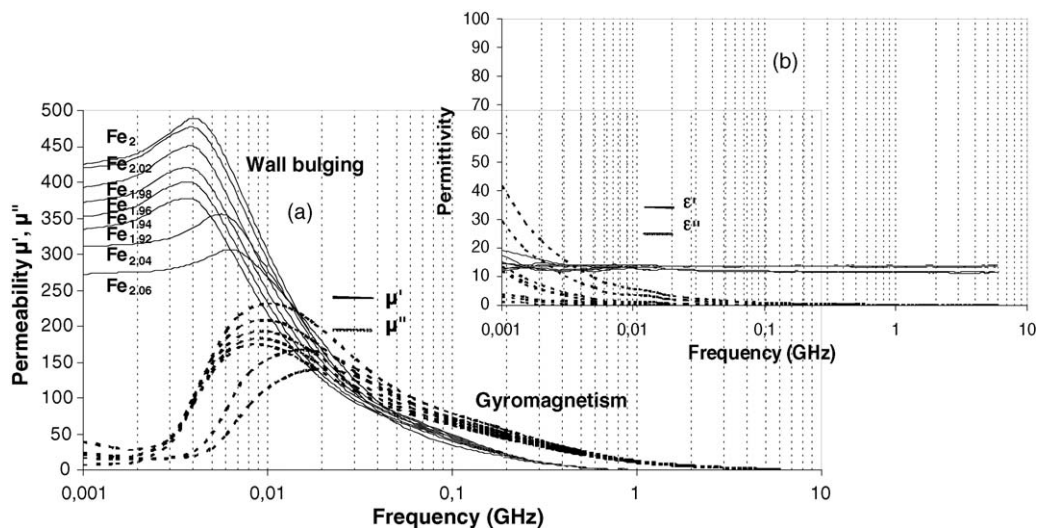


Fig. 10. Permeability (a) and permittivity (b) vs. frequency evolution for different iron stoichiometry,  $\text{Ni}_{0,5}\text{Zn}_{0,5}\text{Fe}_x\text{O}_{4\pm\delta}$  sintered at  $1150^\circ\text{C}$  on toroidal sample.



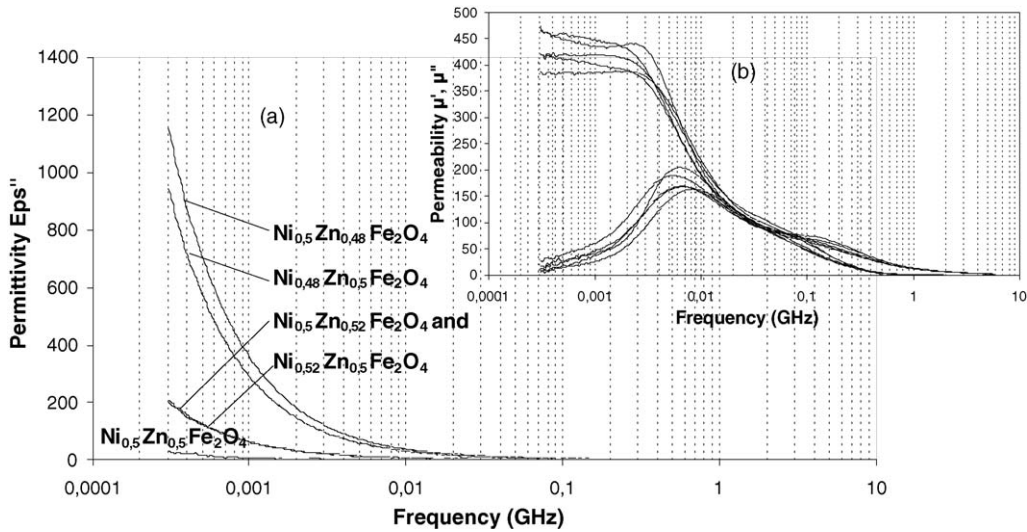


Fig. 11. Permittivity (a) and permeability (b) vs. frequency evolution for different nickel and zinc stoichiometry,  $Ni_xZn_xFe_2O_{4\pm\delta}$  sintered at  $1250^\circ\text{C}$  on toroidal sample.

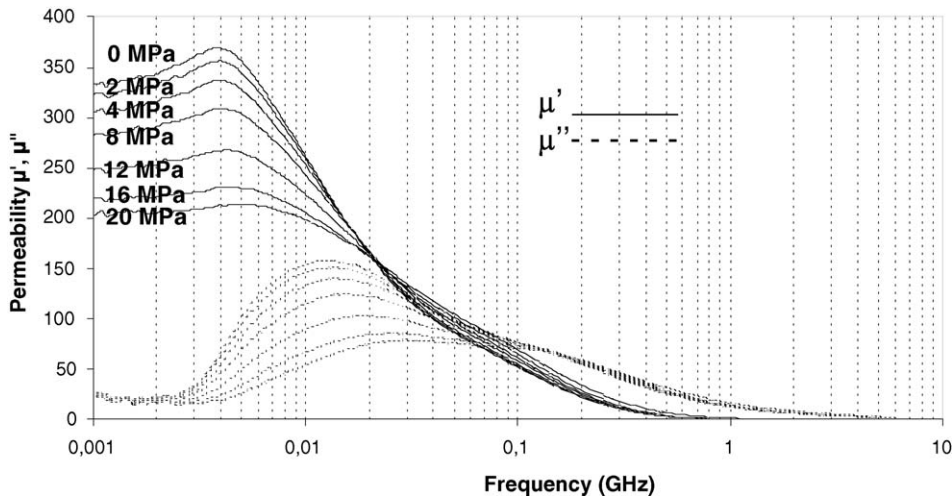


Fig. 12. Permeability vs. frequency for  $Ni_{0.5}Zn_{0.5}Fe_{1.98}O_{4\pm\delta}$  sintered at  $1150^\circ\text{C}$  on toroidal sample and for different applied stresses.

the torus, the magnetization has a tendency to go out of the torus circle because  $Ni_{0.5}Zn_{0.5}Fe_2O_4$  has a negative magnetostriction coefficient (Fig. 13). In this case, it is easy to understand that permeability decreases when the stress increases.

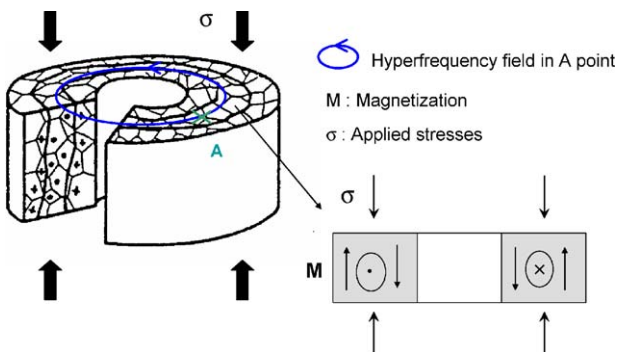


Fig. 13. Magnetic configuration when a stress is applied on a toroidal sample of ferrite with a negative magnetostriction coefficient.

For gyromagnetism, it is well known that the amplitude of the resonance is proportional to the magnetization component perpendicular to the high frequency field. In the case of applied stress, the magnetization has a tendency to go out of torus circle and then the amplitude of the resonance increases with the applied stress as observed on Fig. 12. From a quantitative point of view, we can also explain the permeability behavior in term of anisotropy field. The stress generates a contribution to the anisotropy  $H_a = H_k + \beta\lambda\sigma$ , where  $\beta$  depends on the sample geometry (it is positive in this case). On the other hand,  $\mu$  classically varies as  $M_s/H_a$ , where  $M_s$  is the saturation magnetization and  $H_a$  the anisotropy field. In fact,  $\mu$  varies as  $M_s/(H_k + \beta\lambda\sigma)$ , this is agreement with experimental data because magnetostriction coefficient is negative.

Between these two contributions (gyromagnetism and wall bulging), we can observe a crossing point. At this point, the permeability is not influenced by the applied stress. In fact, the variations of the wall bulging contribution are perfectly compensated by the gyromagnetic ones.

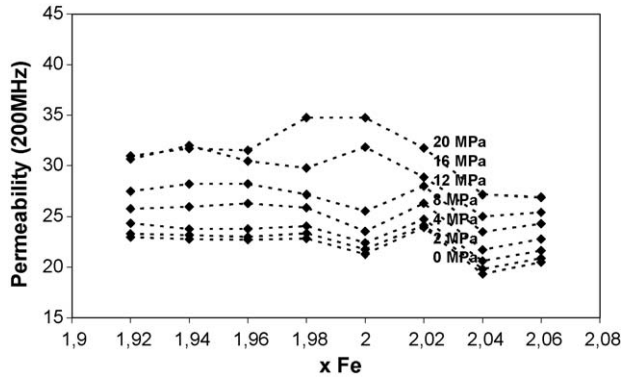


Fig. 14. Permeability (200 MHz) vs. iron stoichiometry for different applied stresses,  $\text{Ni}_{0.5}\text{Zn}_{0.5}\text{Fe}_x\text{O}_{4\pm\delta}$  sintered at  $1150^\circ\text{C}$ .

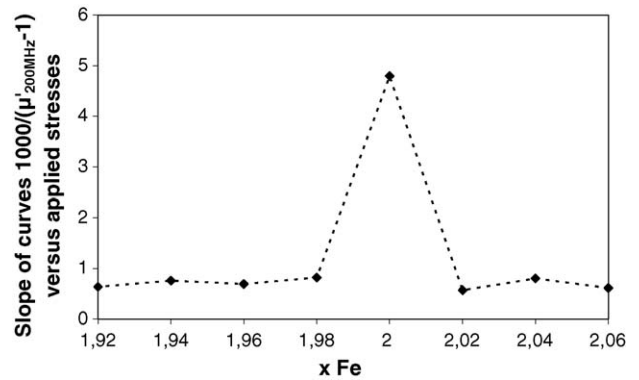


Fig. 17. Slopes of curves  $1000/(\mu'_{200\text{MHz}} - 1)$  vs. applied stresses for iron stoichiometry,  $\text{Ni}_{0.5}\text{Zn}_{0.5}\text{Fe}_x\text{O}_{4\pm\delta}$  sintered at  $1150^\circ\text{C}$ .

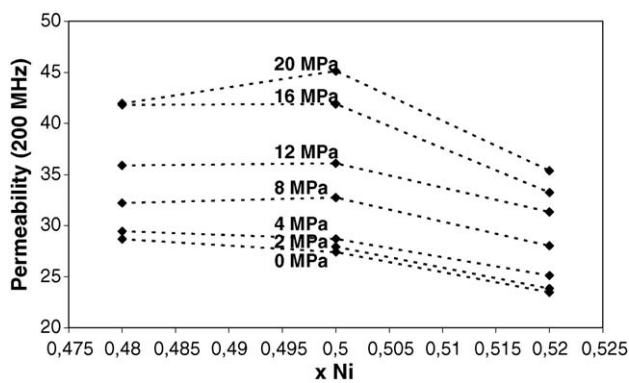


Fig. 15. Permeability (200 MHz) vs. nickel stoichiometry for different applied stresses,  $\text{Ni}_x\text{Zn}_{0.5}\text{Fe}_2\text{O}_{4\pm\delta}$  sintered at  $1250^\circ\text{C}$ .

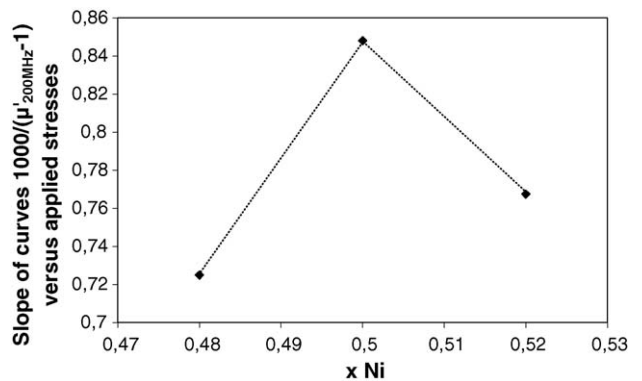


Fig. 18. Slopes of curves  $1000/(\mu'_{200\text{MHz}} - 1)$  vs. applied stresses for nickel stoichiometry,  $\text{Ni}_x\text{Zn}_{0.5}\text{Fe}_2\text{O}_{4\pm\delta}$  sintered at  $1250^\circ\text{C}$ .

To quantify the stoichiometry effect on magneto-elastic properties, we have plotted permeability versus iron (Fig. 14), nickel (Fig. 15) and zinc (Fig. 16) stoichiometry for all applied stresses. This permeability is determined at a frequency of 200 MHz (gyromagnetism).

From 14–16 curves, we can calculate the variations of the inverse permeability ( $1000/(\mu'_{200\text{MHz}} - 1)$ ) versus applied stresses. We obtain a linear curve according to Le Floc'h et al.<sup>8</sup> And in order to obtain stress sensibility, we can plot the slopes of those curves. Results are shown in Figs. 17–19.

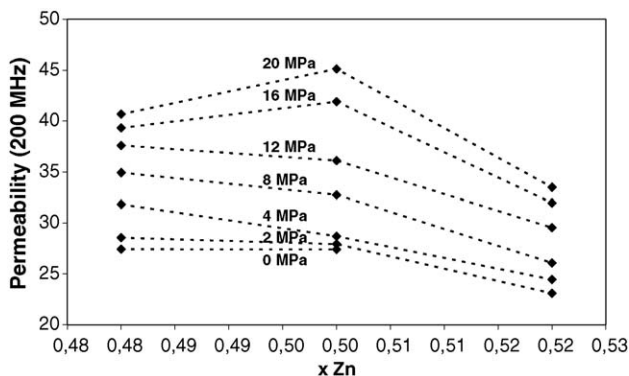


Fig. 16. Permeability (200 MHz) vs. zinc stoichiometry for different applied stresses,  $\text{Ni}_{0.5}\text{Zn}_x\text{Fe}_2\text{O}_{4\pm\delta}$  sintered at  $1250^\circ\text{C}$ .

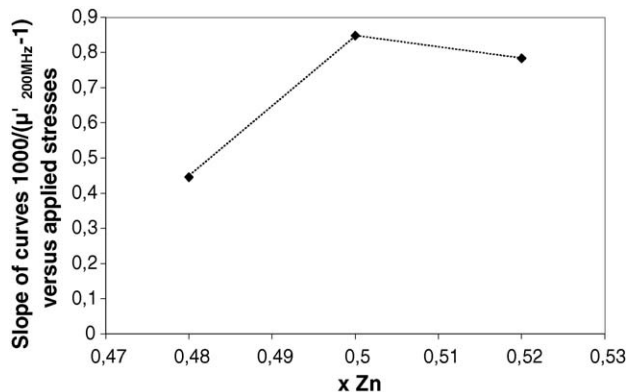


Fig. 19. Slopes of curves  $1000/(\mu'_{200\text{MHz}} - 1)$  vs. applied stresses for zinc stoichiometry,  $\text{Ni}_{0.5}\text{Zn}_x\text{Fe}_2\text{O}_{4\pm\delta}$  sintered at  $1250^\circ\text{C}$ .

Results have a common denominator: stoichiometric materials offer the most important stress sensibility.

## 5. Conclusion

$\text{Ni}_{0.5}\text{Zn}_{0.5}\text{Fe}_2\text{O}_4$  spinel ferrites with variations in Ni, Zn, Fe stoichiometry have been synthesized and characterized. We have clearly shown the linear relation between the lattice parameter and the Curie including all samples. The stoichiometry has an

important influence on permeability versus frequency measurement, with or without stresses. The materials are more sensitive to the stress when they are stoichiometric.

## References

1. Wijn, H. P. J., Gevers, M. and van der Burgt, C. M., Note on the high frequency dispersion in nickel zinc ferrites. *Rev. Modern Phys.*, 1953, **25**(1), 91.
2. Loaëc, J., Le Floc'h, M. and Globus, A., Change of wall topography in soft ferrites by isotropic and anisotropic external pressures. *IEEE Trans. Magnetics*, 1979, **MAG-15**(6), 1861.
3. Stuijts, A. L., Control of microstructures in ferrites. In *Ferrites Proceeding of the International Conference*, Japan, 1970.
4. Globus, A. and Valenzuela Monjaras, R., Influence of the deviation from stoichiometry on the magnetic properties of Zn-rich NiZn ferrite. *IEEE Trans. Magnetics*, 1975, **MAG-11**(5), 1300.
5. Barba, A., Clausell, C., Felúis, C. and Monzó, M., Study of NiZn ferrite complex permeability: effect of relative density and microstructure. *J. Am. Ceram. Soc.*, 2004, **87**(7), 1314.
6. Weiss, Pr., *Phys. Rev.*, 1948, **74**, 1493.
7. Grimal, V., Autissier, D., Longuet, L., Pascard, H., Ledieu, M., Magneto-elastic effect in spinel ferrite. In *Proceeding of Ninth International Conference on Ferrites (ICF-9)*, 2004, p. 359.
8. Le Floc'h, M. and Globus, A., *J. Appl. Phys.*, 1987, **61**(10).